Electronic Supplementary Material (ESI) for Materials Chemistry Frontiers.

Electronic Supplementary Information

Enabling Uniform Li Deposition Behavior with Dynamic Electrostatic Shield by The Single Effect of Potassium Cation Additive for Dendrite-Free Lithium Metal Batteries

Ji Woo Han[a,‡], Bo Keun Park[a,‡], Yong Min Kim[a], Yoonbo Sim[a], Van-Chuong Ho[b], Junyoung Mun[b,c,] and Ki Jae Kim[a,c,]**

[a]Department of Energy Science, Sungkyunkwan University, 2066, Seobu-ro, Jangan-gu, Suwon-si, Gyeonggi-do, 16419, Republic of Korea

[b]School of Advanced Materials Science & Engineering, Sungkyunkwan University, 2066, Seobu-ro, Jangan-gu, Suwon-si, Gyeonggi-do, 16419, Republic of Korea

[c]SKKU Institute of Energy Science and Technology (SIEST), Sungkyunkwan University, 2066, Seobu-ro, Jangan-gu, Suwon-si, Gyeonggi-do, 16419, Republic of Korea

‡ These authors contributed equally to this work

*Corresponding Authors: Junyoung Mun(munjy@skku.edu), Ki Jae Kim

(kijaekim@skku.edu)

Cations	E^0 (V) 1.0 M	Effective reduction potential (V)			
		0.005 M	0.010 M	0.020 M	0.050 M
Li^+	-3.040	·	·	·	·
K^+	-2.931	-3.067	-3.049	-3.032	-3.008

Table S1. Summary effective reduction potentials (vs. standard hydrogen electrode or SHE) of Li^+ and K^+ at different concentrations calculated by the Nernst equation.

Electrolyte composition	**Current Density** ($mA\ cm^{-2}$)	**Areal capacity** ($mAh\ cm^{-2}$)	**Cycle Life** (hours)	**Reference**
1.0 M LiTFSI in DOL/DME/TEGDME (v/v/v = 1:1:2) with 2.0 wt. % $LiNO_3$	1.0	1.0	600	[1]
1.0 M LiTFSI in DOL/DME (v/v = 1:1) with 1.0 wt. % $LiNO_3$ + 5 mM $C_{60}(NO_2)_6$	1.0	1.0	400	[2]
1.0 M LiTFSI in DOL/DME (v/v = 1:1) with 1.0 M Pyr6(6)FSI	1.0	1.0	550	[3]
1.0 M LiTFSI in DOL/DME (v/v = 1:1) with 0.5 wt. % $Im1(8)PF_6$	1.0	1.0	500	[4]
1.0 M LiTFSI in DOL/DME (v/v = 1:1) with 2.0 wt. % Tyr	1.0	1.0	400	[5]
1.0 M LiTFSI in DOL/DME (v/v = 1:1) with 1.0 wt. % $LiNO_3$ + 1.0 wt. % VO79	4.0	1.0	250	[6]
1.0 M LiTFSI in DOL/DME (v/v = 1:1) with 1.0 wt. % $LiNO_3$ + 0.010 M KTFSI	1.0 4.0	1.0 1.0	600 400	**Our works**

Table S2. Comparison of cycling performance for this work with recently reported in the Li symmetric cells.

	R_e (Ω)	R_{SEI} (Ω)	R_{ct} (Ω)	$R_{Interface}$ (Ω)
Pristine	1.58	68.9	26.1	95.0
20th Cycles	2.11	1.84	10.41	12.25
40th Cycles	3.73	2.89	14.40	17.28
60th Cycles	5.61	4.08	20.52	24.60

Table S3. EIS fitting results of the Li | Li symmetric cell with LiTFSI electrolyte.

	R_e (Ω)	R_{SEI} (Ω)	R_{ct} (Ω)	$R_{Interface}$ (Ω)
Pristine	1.37	34.87	57.11	91.98
20th Cycles	1.67	0.90	9.30	10.20
40th Cycles	2.10	1.61	14.99	16.60
60th Cycles	3.91	2.52	14.40	16.92

Table S4. EIS fitting results of the Li | Li symmetric cell with 10 KTFSI electrolyte.

	After 1st Cycle			After 50th Cycles		
	R_e (Ω)	R_{SEI} (Ω)	R_{ct} (Ω)	R_e (Ω)	R_{SEI} (Ω)	R_{ct} (Ω)
LiTFSI	1.62	2.70	50.76	1.27	6.90	131.70
10 KTFSI	1.25	6.72	52.97	1.07	5.47	44.86

Table S5. EIS fitting results of the Li | LFP full cells with two types of electrolytes.

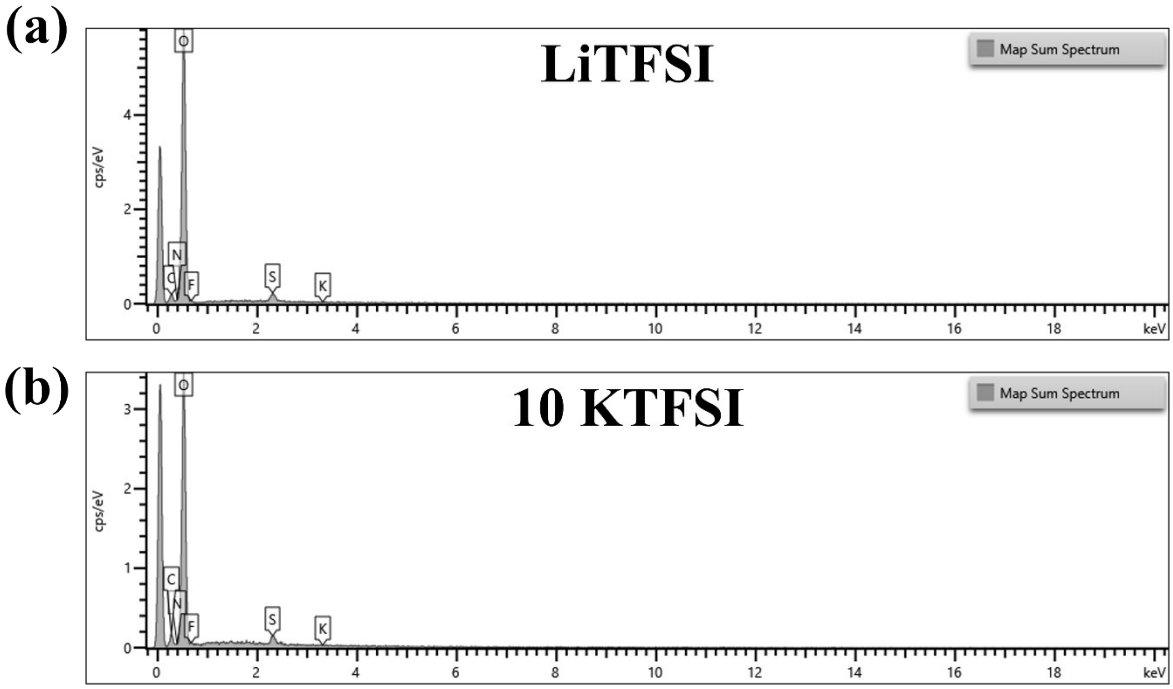

Fig. S1 EDS mapping spectrum of the deposited Li electrode of Li | Li cells from the electrolyte added (a) LiTFSI and (b) 10 KTFSI.

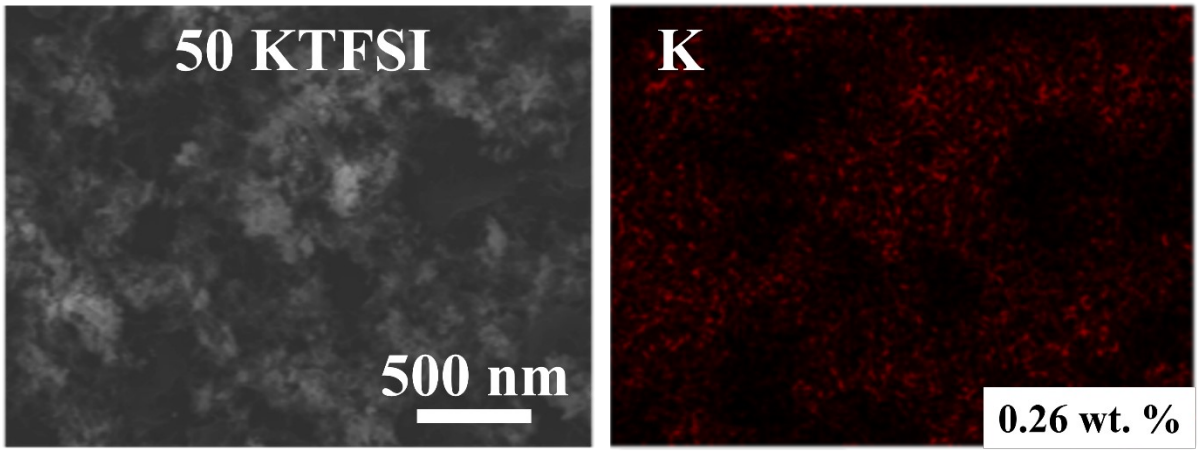

Fig. S2 SEM (left) and EDS potassium mapping images (right) of the deposited Li electrode of Li | Li cells from the electrolyte added 50 KTFSI with weight percent of K element.

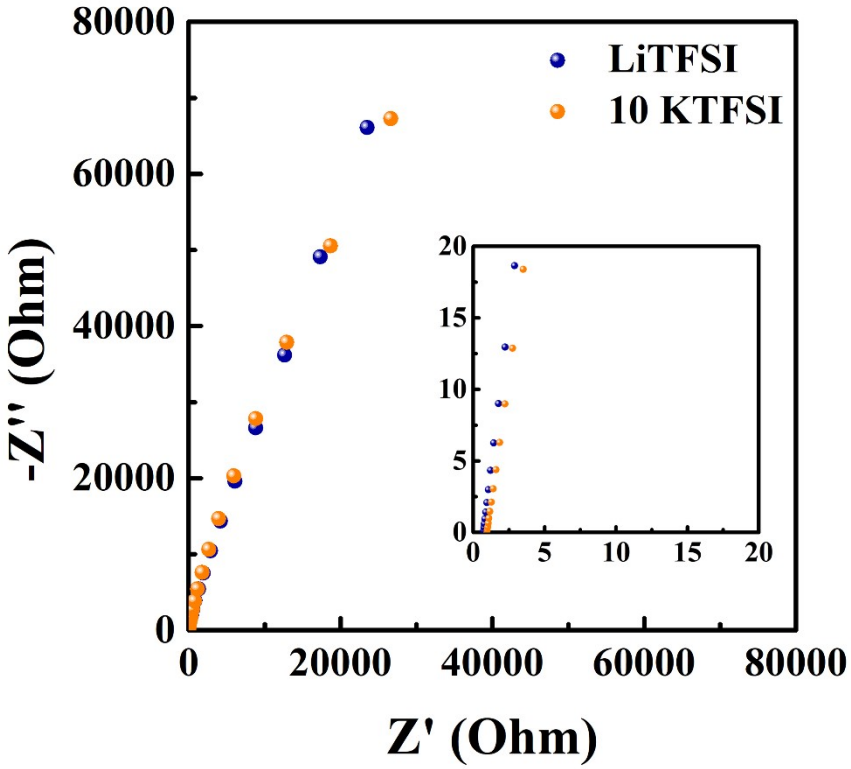

Fig. S3 The EIS plots of cells with and without KTFSI additive at the frequency of 0.1–10^6 Hz, and the cells were assembled by the form of SUS | PE separator | SUS.

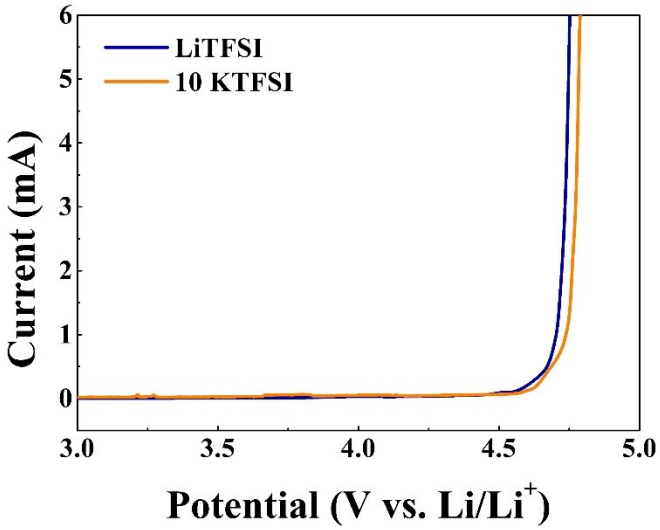

Fig. S4 Linear sweep voltammetry (LSV) curves of with and without KTFSI additive at the scan rate of 1.0 $mV \cdot s^{-1}$ and the cells were assembled by the form of Li | PE separator | SUS.

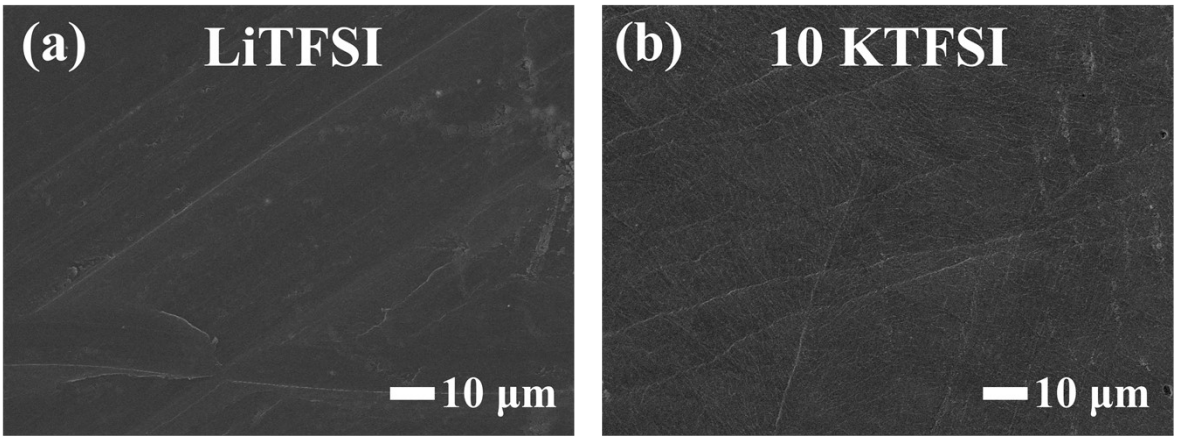

Fig. S5 SEM images of Li metal surface in Li | Cu cells with (a) LiTFSI and (b) 10 KTFSI after storage for 24 hours.

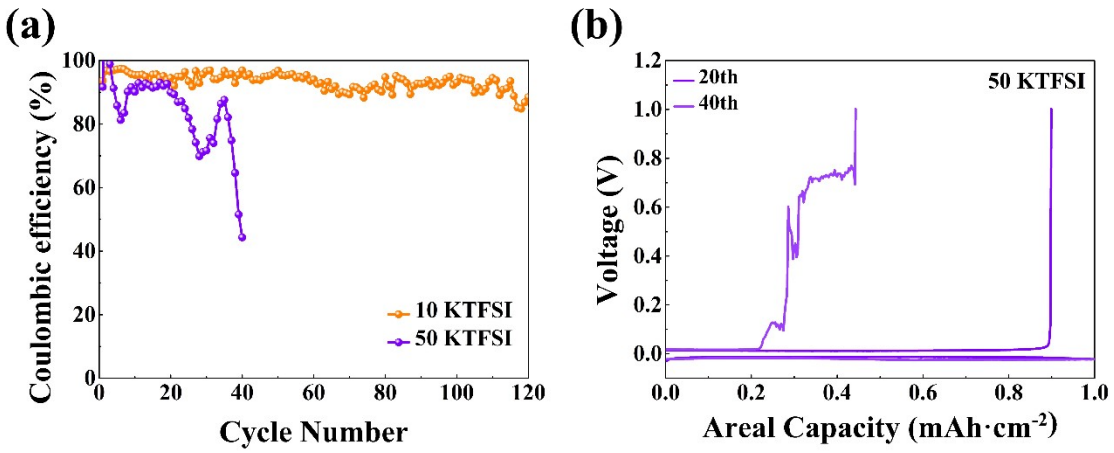

Fig. S6 (a) Comparison of their Coulombic efficiencies over cycling at a current density of 1.0 mA cm^{-2}, and the corresponding Li plating and stripping voltage profiles of (b) 50 KTFSI electrolytes.

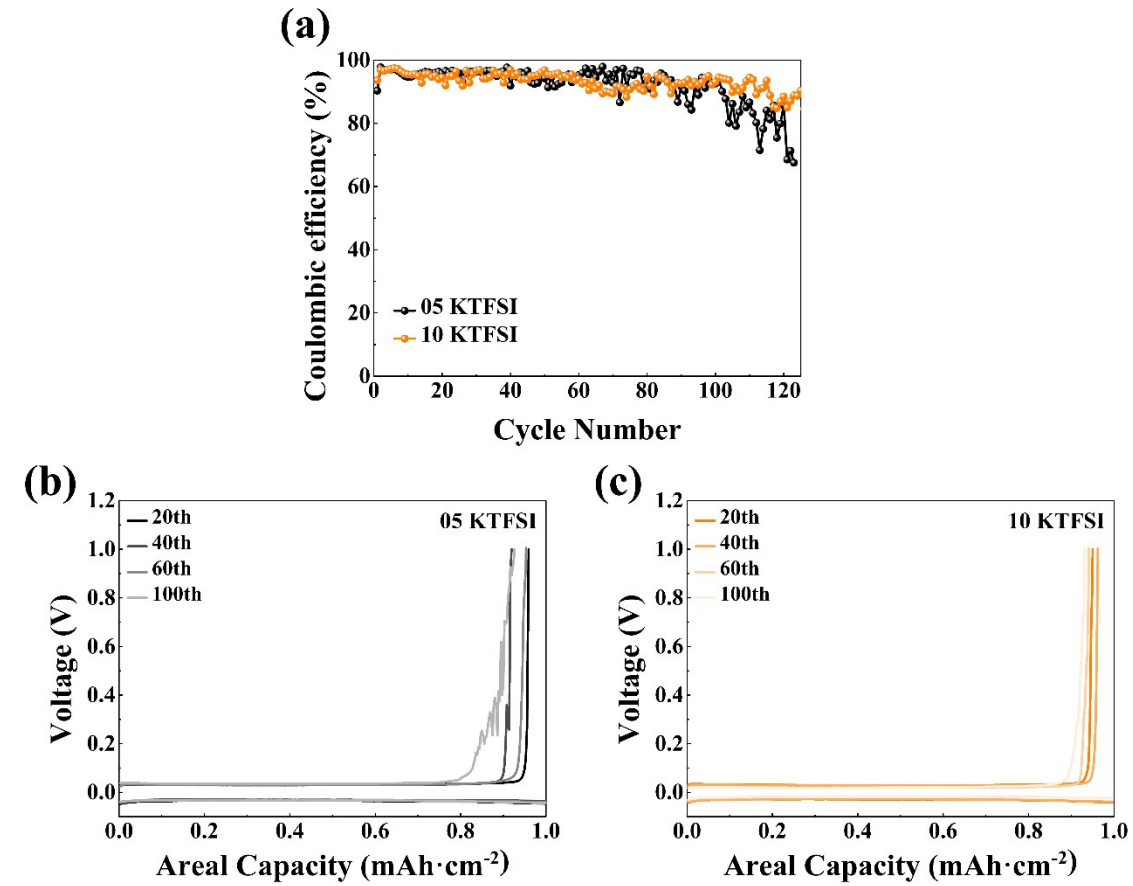

Fig. S7 (a) Comparison of their Coulombic efficiencies over cycling at a current density of 1.0 mA cm^{-2}, and the corresponding Li plating and stripping voltage profiles of (b) 05 KTFSI and (c) 10 KTFSI electrolytes.

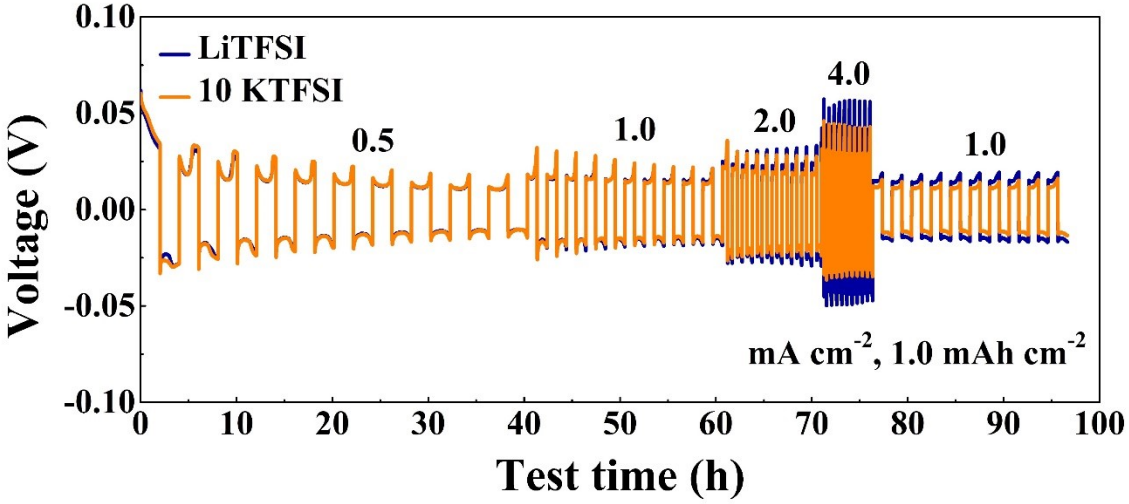

Fig. S8 voltage profile of Li | Li symmetric cells with different electrolytes, Areal capacity = 1.0 mAh cm^{-2}, at different areal current density = 0.5, 1.0, 2.0, 4.0, 1.0 mA cm^{-2}.

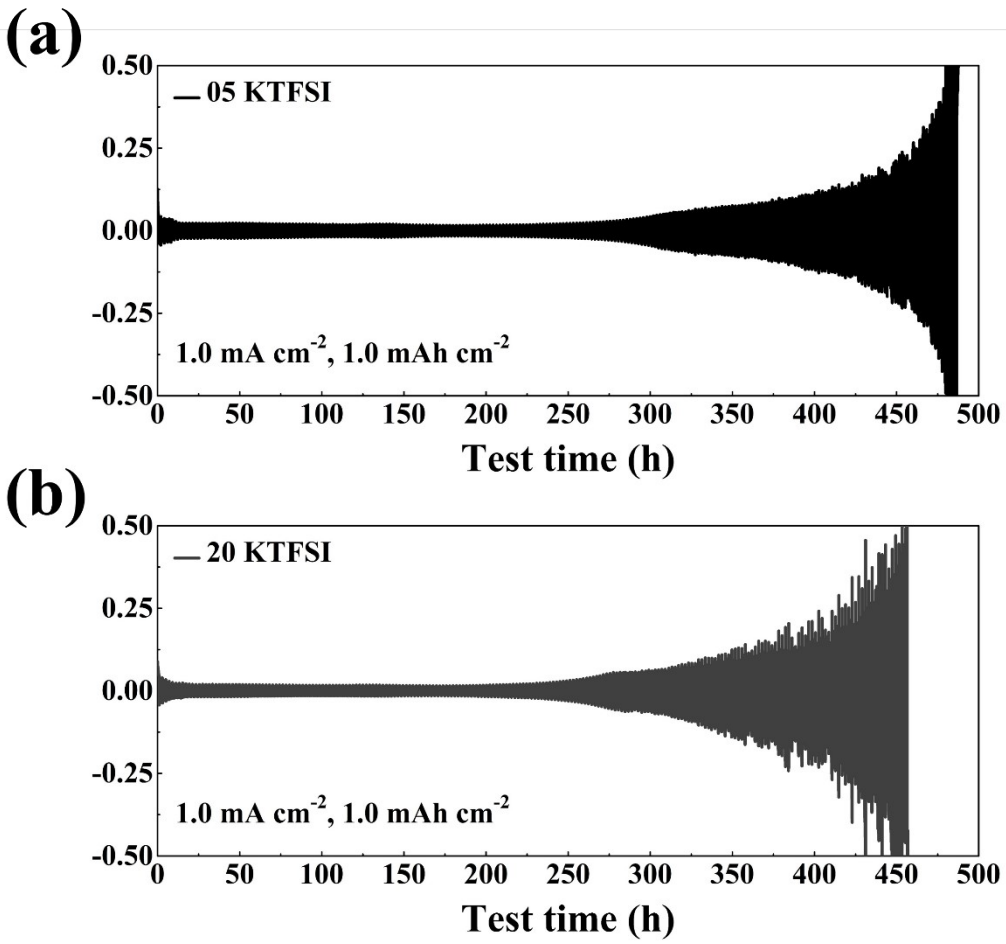

Fig. S9 Galvanostatic Li stripping/plating voltage profiles of symmetric cells with (a) 05 KTFSI and (b) 20 KTFSI at 1.0 mA cm^{-2} with a capacity of 1.0 mAh cm^{-2}.

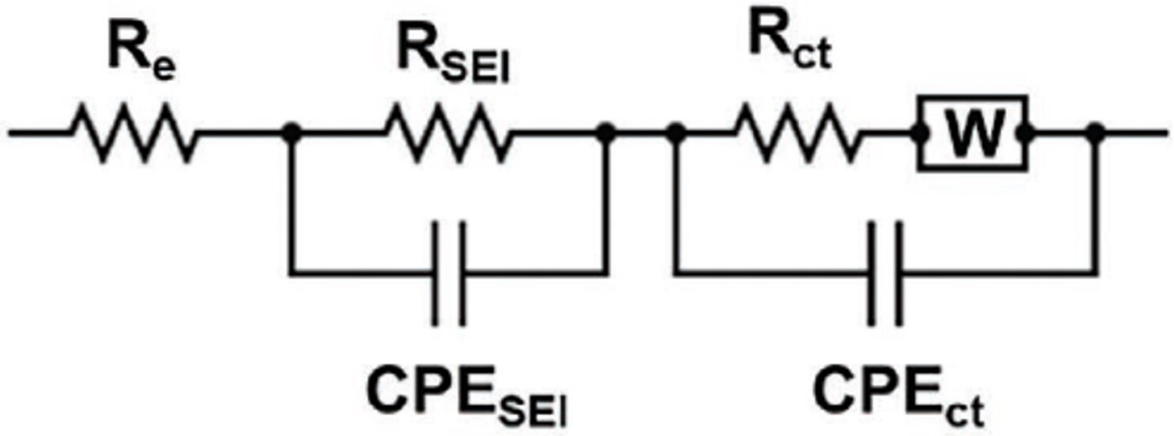

Fig. S10 Equivalent fitting circuit applied to fit the impedance spectra.

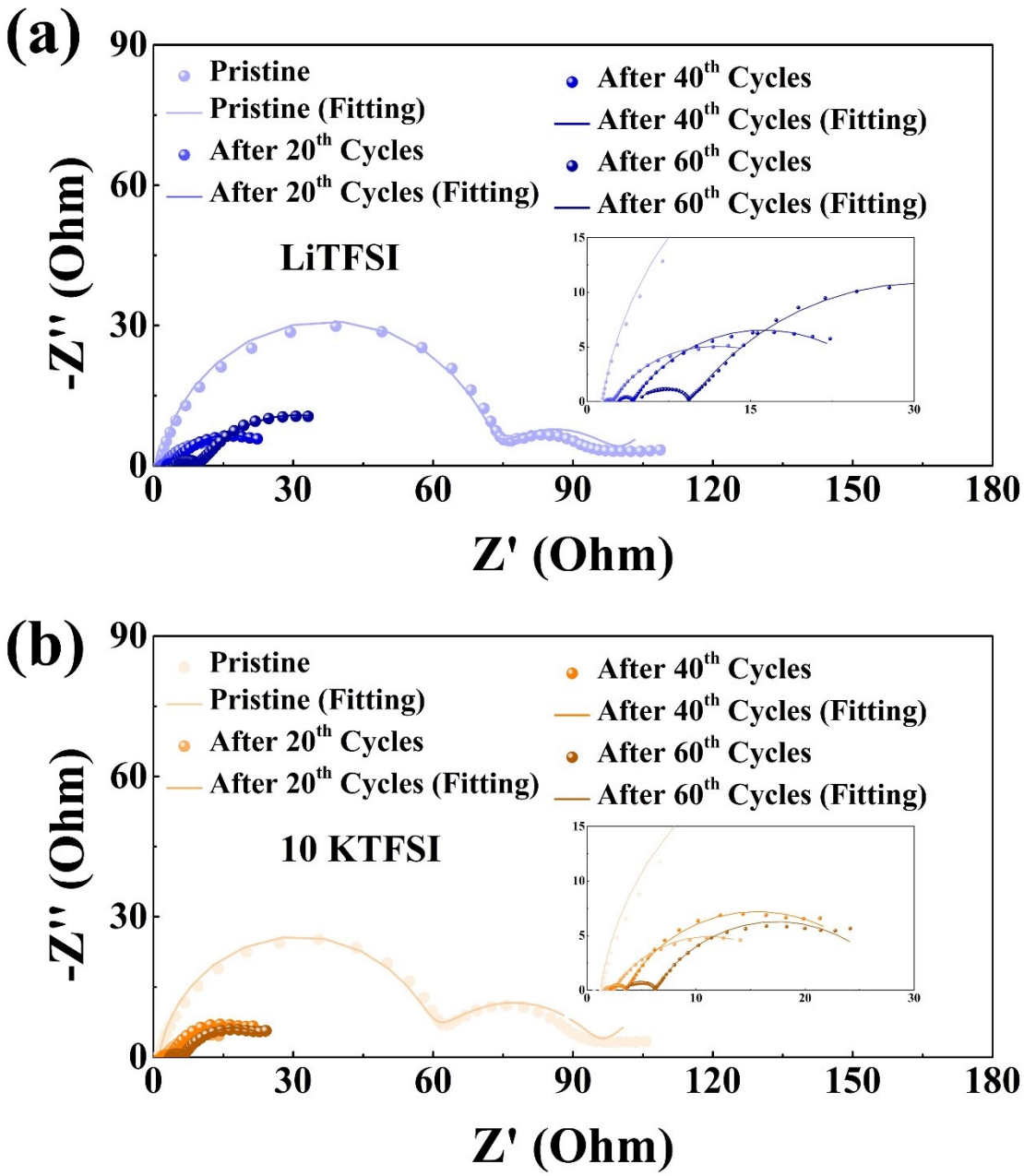

Fig. S11 Nyquist plots of the Li | Li symmetric cells with (a) LiTFSI (b) 10 KTFSI; the inset figure is the magnified view, and the line is the fitting curve.

After 30 cycles

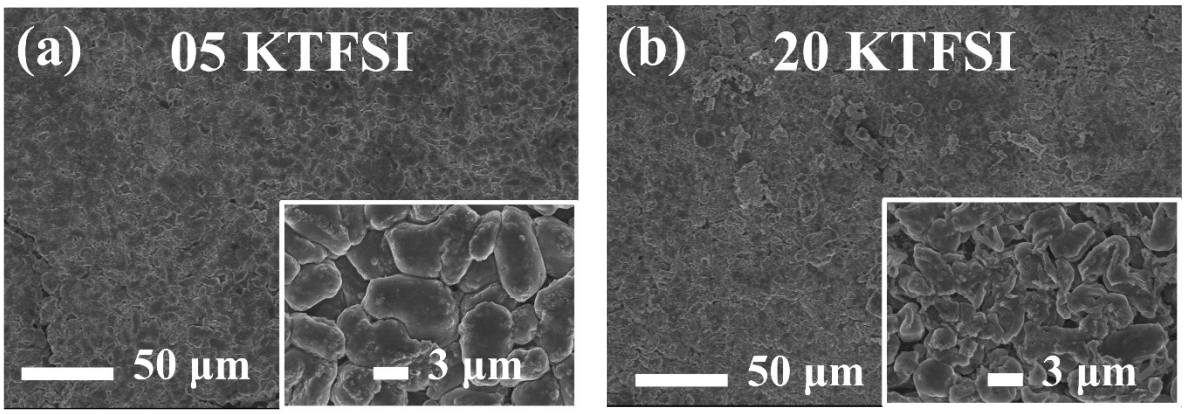

Fig. S12 Top-view SEM images of the lithium deposition morphology: The cell with (a) 05 KTFSI and 20 KTFSI after 30 cycles.

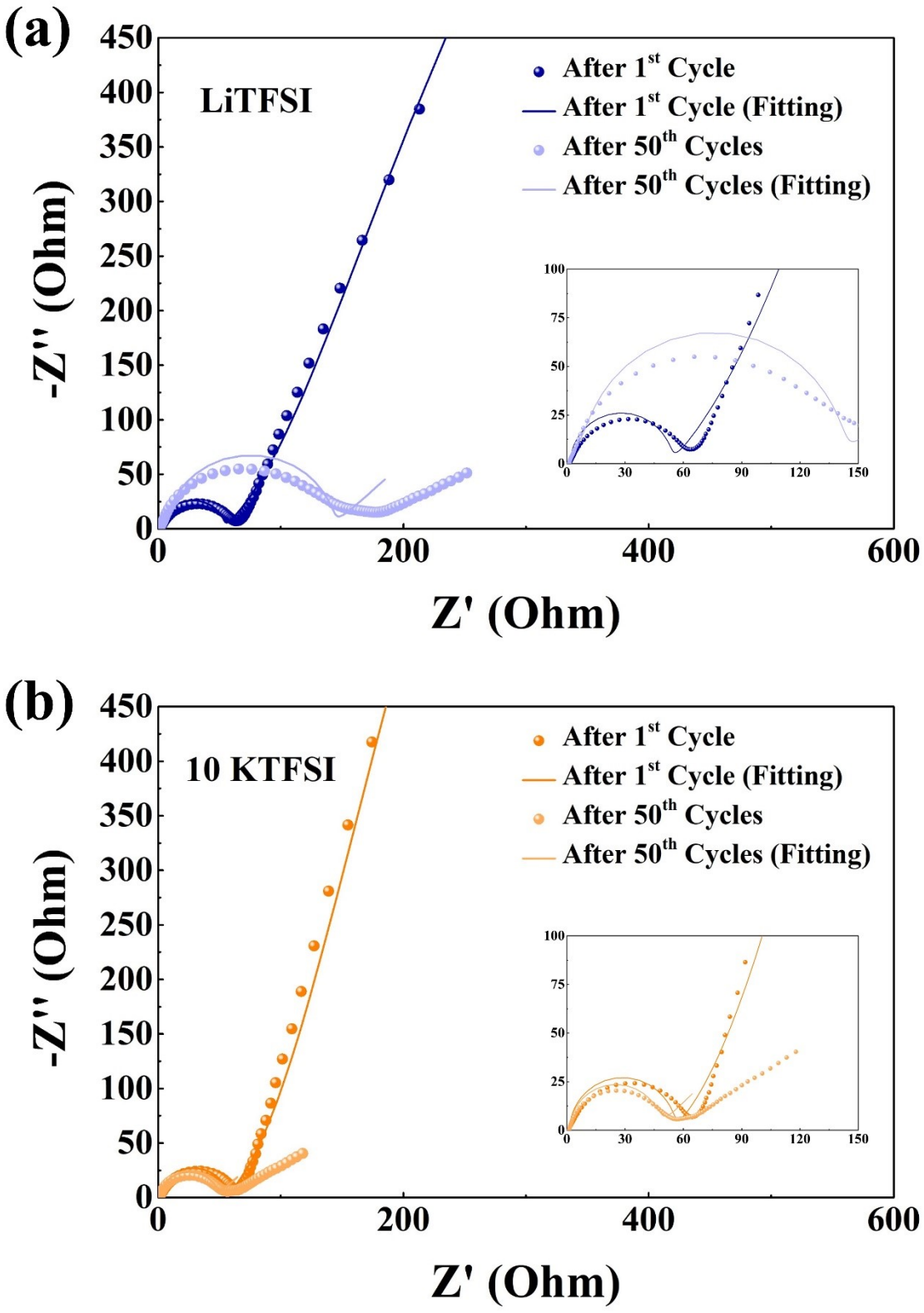

Fig. S13 Nyquist plots of the Li | LFP full cells with a) LiTFSI b) 10 KTFSI; the inset figure is the magnified view, and the line is the fitting curve.

References

[1] H. Yang, L. Yin, H. Shi, K. He, H. M. Cheng and F. Li, Suppressing lithium dendrite formation by slowing its desolvation kinetics, *Chem Commun (Camb)*, 2019, **55**, 13211-13214.

[2] Z. Jiang, Z. Zeng, C. Yang, Z. Han, W. Hu, J. Lu and J. Xie, Nitrofullerene, a C(60)-based Bifunctional Additive with Smoothing and Protecting Effects for Stable Lithium Metal Anode, *Nano Lett*, 2019, **19**, 8780-8786.

[3] J. Jang, J. S. Shin, S. Ko, H. Park, W. J. Song, C. B. Park and J. Kang, Self-Assembled Protective Layer by Symmetric Ionic Liquid for Long-Cycling Lithium–Metal Batteries, *Advanced Energy Materials*, 2022, **12**.

[4] W. Wang, W. Ma, Q. Yang, Z. Lin, J. Tang, M. Wang, Y. He, C. Fan and K. Sun, Imidazolium-Based Ionic Liquid as a Solid Electrolyte Interphase-Forming Additive for Lithium Metal Anodes, *Industrial & Engineering Chemistry Research*, 2022, **61**, 10883-10890.

[5] Z. Chu, S. Zhuang, J. Lu, J. Li, C. Wang and T. Wang, In-situ electro-polymerization of l-tyrosine enables ultrafast, long cycle life for lithium metal battery, *Chinese Chemical Letters*, 2023, **34**.

[6] S. Chang, X. Jin, Q. He, T. Liu, J. Fang, Z. Shen, Z. Li, S. Zhang, M. Dahbi, J. Alami, K. Amine, A. D. Li, H. Zhang and J. Lu, In Situ Formation of Polycyclic Aromatic Hydrocarbons as an Artificial Hybrid Layer for Lithium Metal Anodes, *Nano Lett*, 2022, **22**, 263-270.